

# Searching for p-modes in MOST<sup>★</sup> Procyon data: Another view

F. Baudin<sup>1</sup>, T. Appourchaux<sup>1</sup>, P. Boumier<sup>1</sup>, R. Kuschnig<sup>2</sup>, J.W. Leibacher<sup>1,3</sup>, and J.M. Matthews<sup>2</sup>

<sup>1</sup> Institut d'Astrophysique Spatiale, CNRS/Université Paris XI UMR 8617, F-91405 Orsay, France

<sup>2</sup> Department of Physics and Astronomy, University of British Columbia, 6224 Agricultural Road, Vancouver V6T 1Z1, Canada

<sup>3</sup> National Solar Observatory, 950 N. Cherry Avenue, Tucson AZ 85719-4933, USA

Received ; Accepted

## ABSTRACT

**Context.** Photometry of Procyon obtained by the MOST satellite in 2004 has been searched for p modes by several groups, with sometimes contradictory interpretations.

**Aims.** We explore two possible factors that complicate the analysis and may lead to erroneous reports of p modes in these data.

**Methods.** Two methods are used to illustrate the role of subtle instrumental effects in the photometry: time-frequency analysis, and a search for regularly spaced peaks in a Fourier spectrum based on the echelle diagramme approach.

**Results.** We find no convincing evidence of a p-mode signal in the MOST Procyon data. We can account for an apparent excess of power close to the p-mode frequency range and signs of structure in an echelle diagramme in terms of instrumental effects.

**Key words.** Stars: Procyon – Stars: oscillations

## 1. Introduction

The search for acoustic oscillations in the star Procyon A (which we call hereafter simply Procyon) has been a key part of the young field of stellar seismology for two decades, since the first claim of p-mode detection by Gelly et al. (1986). In recent years, interest grew rapidly with the announcement by Martić et al. (1999) of global acoustic modes in Procyon detected in high-resolution, time-resolved spectroscopy, confirmed by Barban et al. (1999). Interest turned to controversy with the non-detection of intensity oscillations by the MOST (Microvariability & Oscillations of STars) space-borne photometer (Matthews et al. 2004), while contemporaneous groundbased spectroscopic campaigns by Martić et al. (2004), Eggenberger et al. (2004) and Bouchy et al. (2004) appeared to confirm the presence of stellar oscillations. This non-detection triggered considerable speculation about non-stellar noise sources in the MOST data (Christensen-Dalsgaard & Kjeldsen 2004; Bedding et al. 2005) and independent analyses of those data claiming possible evidence for p modes, but using different analysis methods (Régulo & Roca Cortés 2005; Garcia et al. 2007). The contrast between the reported p-mode signal in lu-

minosity and integrated radial velocity also inspired theorists to refine models of convection and turbulence in Procyon (e.g., Robinson et al. 2005).

The MOST team has described the nature of the Fabry Imaging data on which the Procyon photometry is based (Reegen et al. 2006), including the recognised effects of stray light due to Earthshine modulated by the MOST satellite orbit and a beating effect of the science and startracker CCD timing in the early stages of the mission.

We present an independent analysis of the MOST Procyon data compared to simulations, calling attention to how the timing effects and orbital artifacts can be misinterpreted as evidence for p-mode oscillations.

## 2. Time-frequency analysis

The 32-day-long MOST photometric time series has a duty cycle of 99% (for more details, see Matthews et al. 2004). This continuity of the data, currently unique to MOST observations of stars and a key element of the motivation for future photometric space missions such as CoRoT and Kepler, has many important advantages. It eliminates the cycle/day aliases common to groundbased campaigns, even with multiple sites. Another benefit, which we exploit in this paper, is that these data make it possible to investigate variation of the frequency content of the signal as a function of time more sensitively than for other astronomical data sets.

We have applied a time-frequency analysis, based on a Morlet

Send offprint requests to: F. Baudin, frederic.baudin@ias.u-psud.fr

<sup>★</sup> Based on data from the MOST satellite, a Canadian Space Agency mission, jointly operated by Dynacon Inc., the University of Toronto Institute for Aerospace Studies and the University of British Columbia, with the assistance of the University of Vienna.

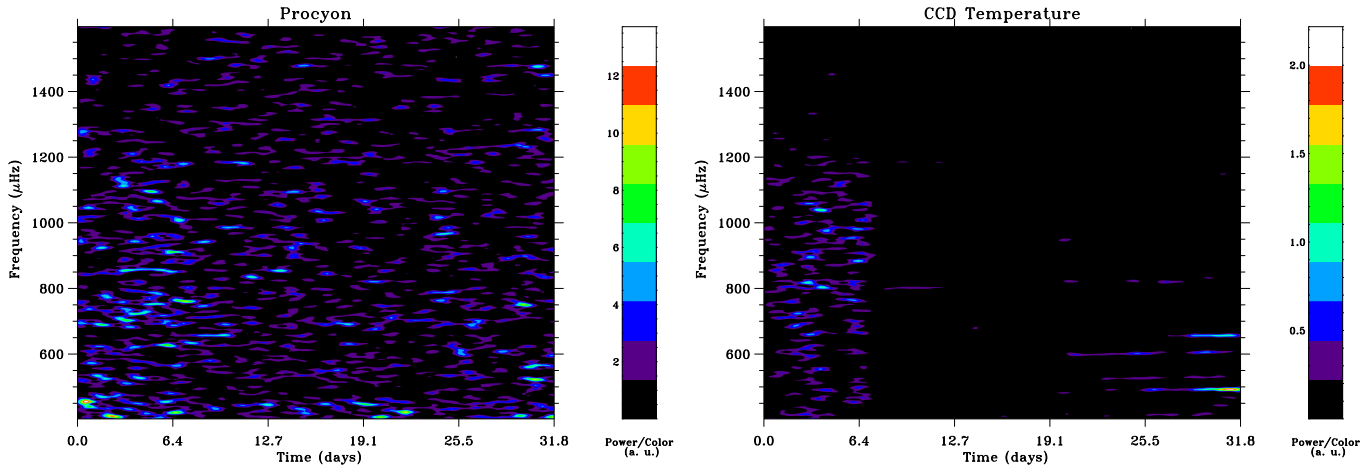


**Fig. 1.** Left: Time/frequency diagramme of Procyon data, showing excess power between 500 and 1200  $\mu\text{Hz}$  during the first eight days of observation. Right: same analysis of the CCD temperature, showing the same excess of power

wavelet (see Baudin *et al.* 1994), to the time series of the MOST photometry and to time series of instrumental parameters such as satellite pointing error and CCD temperature, which are included in the MOST science telemetry. The left-hand panel of Figure 1 shows the distribution of power in the MOST Procyon photometry as a function of both frequency and time. There is some excess power during the first 8 days of the observations, in the frequency range of about 500–1200  $\mu\text{Hz}$ . The contrast in excess power is small and can be seen more clearly when the power is summed over frequency as a function of time, as shown in Figure 2. The average increase in the excess power is about 35%. The same time-frequency analysis was applied to time series of spacecraft and instrument parameters in the MOST science telemetry. Some (but not all) temperatures measured on board seem to show an excess of power in the same ranges of time and frequency as in the stellar light curve. The time-frequency plot of the MOST science CCD temperature is shown in the right-hand panel of Figure 1. Other parameters, such as telescope-pointing wander, do not show such behaviour. However, this does not mean that on board temperature variations are the cause of the observed photometric power excess. MOST CCD temperatures (operating at around  $-35^\circ\text{C}$ ) are controlled to within  $0.1^\circ\text{C}$  and are monitored to an accuracy of  $0.01^\circ\text{C}$ . The very small amplitude of the temperature variations is insufficient to change the dark current or other characteristics of the CCD output to account for the excess seen in Figure 2. Furthermore, there is no one-to-one correlation in time and frequency. More likely, both the temperature and photometric variations are symptoms of a common cause. There is nothing in the MOST operations records or in other telemetry that can explain such a change on the seventh day of the observations. Among the different instrumental effects described by Reegen *et al.* (2006), none seems to be clearly the cause of this observation. However, one must note that these seven days represent the first seven days of science operations of the MOST satellite.

The smoothed Fourier spectrum of the first seven days of the Procyon photometry shows greater spectral power density up to

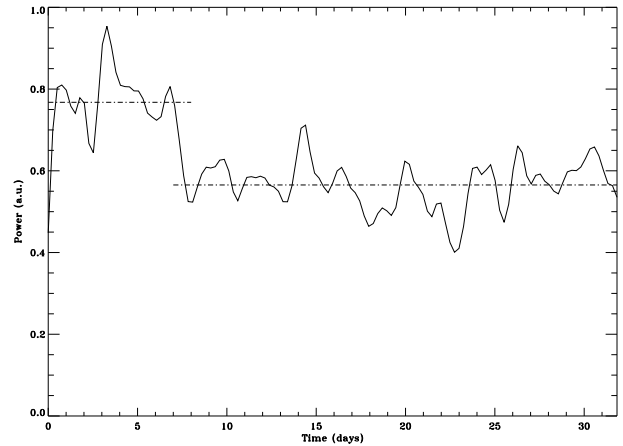


**Fig. 2.** Time variation of the integrated power (from 400 to 1600  $\mu\text{Hz}$ ), showing two different levels during the observations.

about 1200  $\mu\text{Hz}$  than during the remaining 24 days (Figure 3). This includes the frequency range where acoustic vibrations of the star are anticipated, both from theory and the spectroscopic observations. Therefore, this power contrast must be taken into account in any analysis looking for p modes, which should be sought preferentially in the second part of the photometric time series.

### 3. Collapsed echelle diagramme analysis

The acoustic spectrum of a star such as Procyon is expected to have modes with a roughly regular spacing in frequency (called the “large spacing”  $\Delta_0$ ). One way to see this spacing (as well as fine spacings between modes) is to construct an echelle diagramme (Grec 1981), widely used in helio- and asteroseismology. This is done by cutting the Fourier spectrum into  $N_c$  frequency intervals of width  $\Delta$ , and then plotting each interval above the previous one, such that the  $x$ -axis is the frequency modulo  $\Delta$  and the  $y$ -axis is the frequency. The regular spac-

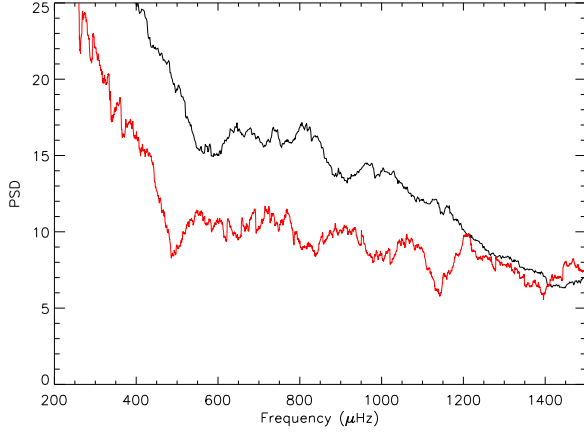


**Fig. 3.** Smoothed Fourier spectra of Procyon data for the first seven days (black) and last 25 days (red) of observation

ing of modes in the asymptotic regime yields clear, nearly vertical, ridges in the echelle diagramme. To enhance the signal-to-noise ratio (SNR) in an echelle diagramme, it is possible to collapse the second dimension (the order of the echelle) as proposed by Korzennik (2007). If the spacing  $\Delta$  chosen is the actual large spacing  $\Delta_0$  of the p-mode eigenspectrum of the star, then a peak should appear or become clearer in this “collapsed echelle diagramme”. To search for a p-mode spacing in data of low SNR, this can be repeated for a set of  $\Delta$  values and a 2D collapsed echelle diagramme can be constructed. The resulting diagramme, built with prewhitened spectra (by dividing the original spectra by the smoothed  $-200 \mu\text{Hz}$  window– spectra), is normalised as follows:

$$P(\nu) = \left( \frac{p(\nu)}{2N_c S_f} - 1 \right) / s \quad (1)$$

where  $s$  is a detection level defined below,  $P(\nu)$  is the normalized, collapsed echelle diagramme;  $p(\nu)$  is the original collapsed echelle diagramme having a  $\chi^2$  with  $2N_c S_f$  degrees of freedom,  $N_c$  being the number of frequency intervals collapsed; and  $S_f$  is the smoothing factor used, if any. The normalisation factor ( $2N_c S_f$ ) in Equation 1 allows one to compensate for the varying number of degrees of freedom in the collapsed echelle diagramme.

We first set the *a priori* detection probability such that we can derive the detection level  $s$  using the cumulative probability for the statistics mentioned above. The detection level  $s$  (Appourchaux 2004, Equation 1) is then given by:

$$\mathcal{P}(s' \geq s, q) = \int_s^{+\infty} \frac{1}{\Gamma(q)} \frac{u^{q-1}}{S^q} e^{-u/S} du \quad (2)$$

with  $q = N_c S_f$  and  $S$  is the mean noise level in the power spectrum. The detection level ( $s$ ) is set *a priori* to be 1%, *i.e.* there is a one percent chance that in a window of width  $N_w$  bins, a peak due to noise will be higher than the level  $s$ . When there is no smoothing factor, the number of independent bins is  $N_w$ . When a smoothing factor is applied, the number of independent bins decreases linearly with the smoothing factor. The level  $s$

for a single bin is then obtained by solving the following equation:

$$\mathcal{P}(s' \geq s, q) = 0.01 \frac{S_f}{N_w} \quad (3)$$

This approximation is valid because the probability of 1% is small compared to one.

It should be noted that if a spacing  $\Delta_0$  exists in the spectrum, a different spacing  $\Delta'_0$  defined as

$$m\Delta'_0 = n\Delta_0, \quad (4)$$

with  $m$  and  $n$  being integers, will also be observed in an echelle diagramme. This artifact plagues any technique based on the detection of regularly-spaced peaks.

We apply this method to simulated data in the next subsection, in the framework of preparation for the CoRoT mission (see Appourchaux *et al.* 2006) in order to detect low-SNR modes with a regular frequency spacing. We then apply it to the MOST Procyon photometry.

### 3.1. Simulated data

The simulated data used here (see Baudin *et al.* 2006) include an estimate of the granulation noise (the dominant component of the intrinsic stellar noise in the p-mode frequency range) and theoretically predicted p-mode amplitudes. The granulation noise is modelled in a simple way (a Lorentzian shape in the Fourier spectrum) and the modes’ amplitudes are based on Samadi *et al.* (2003). These amplitudes can be attenuated or enhanced in order to produce a desired SNR. In the simulations here, we set the mode SNR (defined as  $(P_{\text{mode}} + P_{\text{noise}})/P_{\text{noise}}$ ) to be 1.3. The input frequencies of the simulated modes correspond to a mean large spacing of  $\Delta_0 = 82 \mu\text{Hz}$ , with a standard deviation of  $\approx 2.3 \mu\text{Hz}$ . A smoothing factor corresponding to  $\approx 3 \mu\text{Hz}$  has been used. Figure 4 shows the collapsed echelle diagramme for this simulation in which clear peaks above the normalised value of 1.0 (indicating a 99% confidence level) appear for regularly-spaced frequencies having  $\Delta \approx 41, 82, 123, \text{ and } 165 \mu\text{Hz}$ . These correspond to the input value of the large spacing  $\Delta_0$  and the corresponding values  $\Delta'_0$  (defined in Equation 4), demonstrating the strong potential of this approach.

### 3.2. MOST Procyon data

The same type of collapsed echelle diagrammes (with the same smoothing factor) were computed for the MOST Procyon photometry. They have also been applied to the window function of the MOST time series to assess its influence on the analysis. The gaps in the data represent only 7.5 hours in a total observation of 32 days. This is illustrated by the window function (see Fig.5) in which the presence of very short gaps which occur with some periodicity (related to the satellite orbit), induces very weak peaks. Despite their weakness, the regular spacing of these peaks in the Fourier spectrum can interfere with the search for regularly-spaced p modes in this spectrum. The left-hand panel of Figure 6 shows the collapsed echelle diagramme of the window function for the region of the Fourier spectrum

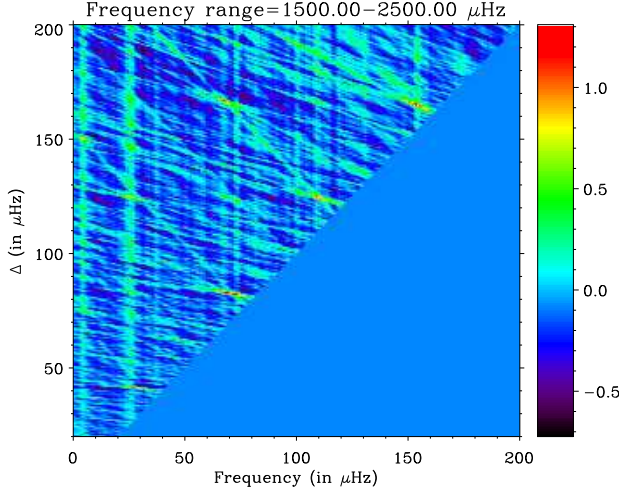


**Fig. 4.** Collapsed echelle diagramme for simulated data, showing the signature of regular spacing of  $\approx 82 \mu\text{Hz}$  and multiples of this spacing as defined in Equation 4

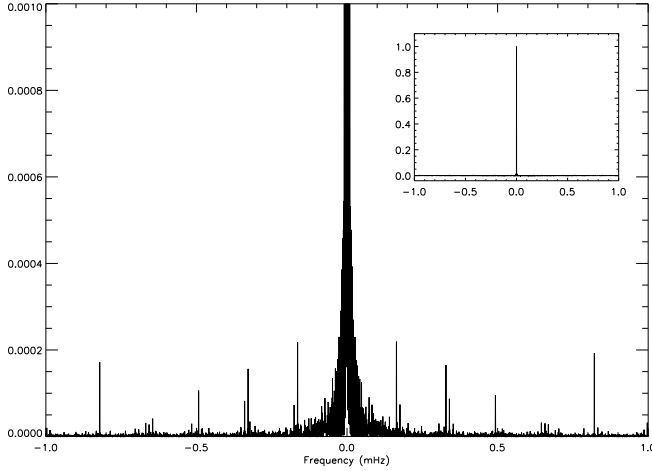


**Fig. 5.** Power spectrum of the window function of the observation, almost perfect but presenting some weak but regularly-spaced peaks

where stellar p modes are expected. One can see clear vertical and oblique structures: the vertical ones are due to large peaks (whatever their origin) in the first frequency interval used to build the diagramme, and the oblique ones to similar large peaks, present in subsequent frequency intervals. Clear peaks above the 99% confidence level appear at  $\approx 165$ , 110, 83, and  $55 \mu\text{Hz}$ . The first of these frequencies is the orbital frequency of the MOST mission (1/101.4 minutes). The other three frequencies correspond to the values of  $\Delta'_0$  for  $(n = 2, m = 3)$ ,  $(n = 1, m = 2)$  and  $(n = 1, m = 3)$  respectively, taking  $165 \mu\text{Hz}$  as  $\Delta_0$  in Equation 4.

The same analysis was performed for the photometric time series. The result, shown in the right-hand panel of Figure 6, shares the dominant pattern with the 2D collapsed echelle of the window function, with ridges at the satellite orbital frequency and for the frequency spacing defined by Equation 4. Figure 7 shows enlarged views of the panels in Figure 6, high-

lighting a small frequency range around  $55 \mu\text{Hz}$ , which is very close to  $1/3$  of the orbital frequency of MOST. A simple echelle diagram or comb analysis may yield some signal at this frequency spacing which is not due to asymptotic p modes in Procyon but rather the intrinsic modulation of stray light background in the photometry.

#### 4. Conclusion

From the two approaches presented here, one can draw two conclusions. First, the Procyon MOST light curve obtained in 2004 shows some changes in the spectral power content after about seven days of observation (which were the first seven days of observation of the MOST mission) that covers the frequency range relevant to the p-mode search and thus requires special care in this search. A counterpart to this change in the CCD temperature telemetry indicates that it is not intrinsic to Procyon.

Second, the echelle-diagramme technique must be applied to Procyon MOST data with care. Despite an excellent observation window, the orbital artifacts in the data introduce apparent spacings close to the p-mode spacing expected for Procyon even though the gaps are very short and their signature in the window spectrum is very weak. However, they are unexpectedly not negligible when searching for regularly-spaced peaks in the Fourier spectrum, reinforcing the need for a careful analysis when looking for regular spacings in the signal spectrum even in the case of a very good observation window.

In conclusion, we do not find any evidence for a stellar oscillation signal in the MOST photometry, and the issue of the nature of luminosity oscillations in Procyon remains open.

*Acknowledgements.* T.A. wishes to thank M. Martić and S. Korzennik for helpful discussions. J.M.M. acknowledges funding from the Natural Sciences & Engineering Research Council (NSERC) Canada. R.K. is supported by the Canadian Space Agency (CSA).

#### References

- Appourchaux, T. 2004, *A&A*, 428, 1039
- Appourchaux, T., Berthomieu, G., Michel, E., et al. 2006, in *ESA SP-1306: The CoRoT Mission*, ed. M. Fridlund, A. Baglin, J. Lochard, & L. Conroy, 377
- Barban, C., Michel, E., Martic, M., et al. 1999, *A&A*, 350, 617
- Baudin, F., Gabriel, A., & Gibert, D. 1994, *A&A*, 285, L29
- Baudin, F., Samadi, R., Appourchaux, T., & Michel, E. 2006, in *ESA SP-1306: The CoRoT Mission*, ed. M. Fridlund, A. Baglin, J. Lochard, & L. Conroy, 403
- Bedding, T. R., Kjeldsen, H., Bouchy, F., et al. 2005, *A&A*, 432, L43
- Bouchy, F., Maeder, A., Mayor, M., et al. 2004, *Nature*, 432, 7015
- Christensen-Dalsgaard, J. & Kjeldsen, H. 2004, *Nature*, 430, 29
- Eggenberger, P., Carrier, F., Bouchy, F., & Blecha, A. 2004, *A&A*, 422, 247
- Garcia, R., Lambert, P., Ballot, J., et al. 2007, *A&A*, submitted
- Gelly, B., Grec, G., & Fossat, E. 1986, *A&A*, 164, 383



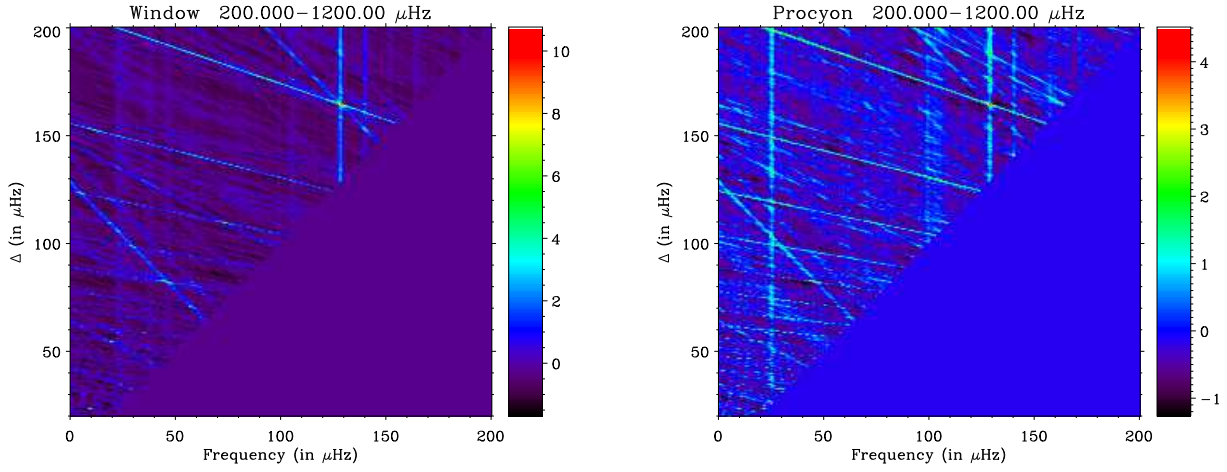


**Fig. 6.** Left: Collapsed echelle diagramme for the Procyon window function. It is dominated by a peak at  $\approx 165 \mu\text{Hz}$  corresponding to the orbital frequency, and other peaks following Equation 4. Right: Same diagramme for Procyon data, with similar patterns

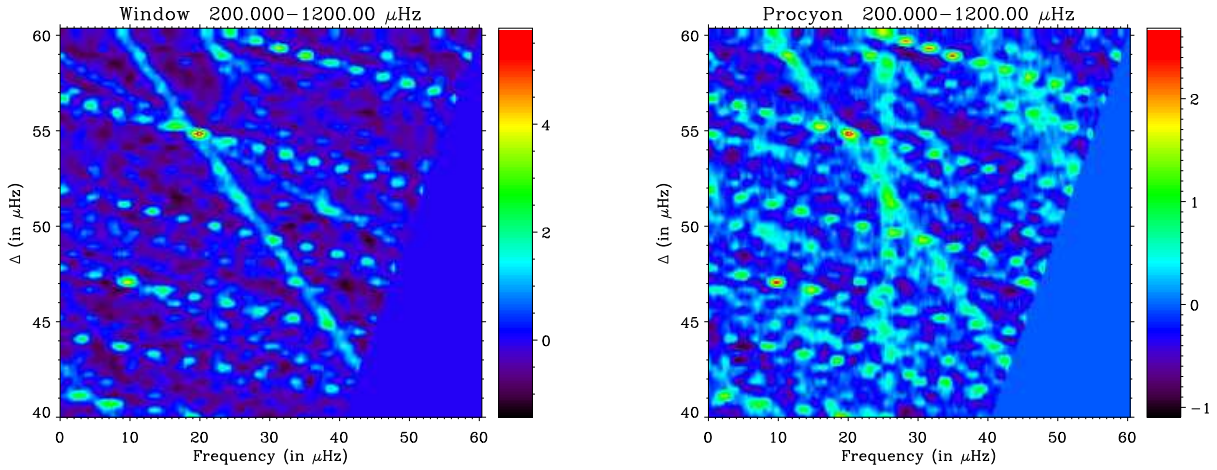


**Fig. 7.** Respective enlargements of the Figure 6. The discontinuous appearance is due do the discrete frequency sampling of the spectra.

- Grec, G. 1981, Ph.D (Université de Nice)  
 Korzennik, S. 2007, Adv. Spa. Res., in press  
 Martić, M., Lebrun, J.-C., Appourchaux, T., & Korzennik, S. G. 2004, A&A, 418, 295  
 Martić, M., Schmitt, J., Lebrun, J.-C., et al. 1999, A&A, 351, 993  
 Matthews, J. M., Kusching, R., Guenther, D. B., et al. 2004, Nature, 430, 51  
 Reegen, P., Kallinger, T., Frast, D., et al. 2006, MNRAS, 367, 1417  
 Régulo, C. & Roca Cortés, T. 2005, A&A, 444, L5  
 Robinson, F. J., Demarque, P., Guenther, D. B., Kim, Y.-C., & Chan, K. L. 2005, MNRAS, 362, 1031  
 Samadi, R., Nordlund, Å., Stein, R. F., Goupil, M. J., & Roxburgh, I. 2003, A&A, 404, 1129